

Gaussian Process Single Index Models for Conditional Copulas

Evgeny Levi

Department of Statistical Sciences, University of Toronto
and

Radu V Craiu

Department of Statistical Sciences, University of Toronto

December 3, 2024

Abstract

Parametric conditional copula models allow the copula parameters to vary with a set of covariates according to an unknown calibration function. In this paper we develop a flexible Bayesian method to estimate the calibration function of a bivariate conditional copula. We construct a prior distribution over the set of smooth calibration functions using a sparse Gaussian process (GP) prior for the single index model (SIM). The estimation of parameters from the marginal distributions and the calibration function is done jointly via a Markov Chain Monte Carlo algorithm that is used to sample from the full posterior distribution. We introduce a novel Conditional Cross Validated Pseudo-Marginal (CCVML) criterion that is used along with the Deviance Information Criterion (DIC), the Watanabe-Akaike Information criterion (WAIC) and the regular Cross-Validated Pseudo-Marginal Likelihood (CVML) criterion to perform copula selection and to compare the full model to one with constant calibration function. The performance of the estimation method and model selection criteria is studied via a series of simulations using correct and misspecified models with Clayton, Frank and Gaussian copulas and a real weather data example.

Keywords: Bayesian inference, Cross-validated Marginal Likelihood, Deviance Information Criterion, Markov chain Monte Carlo, Watanabe-Akaike Criterion.

1 Introduction

Copulas are useful in modelling dependent structures in models in which none of the few available multivariate distributions is suitable. In situations in which all variables involved have continuous marginal distributions, Sklar's theorem (Sklar, 1959) guarantees the existence and uniqueness of the copula $C : [0, 1]^p \rightarrow [0, 1]$ that yields the true joint distribution, i.e. $H(Y_1, \dots, Y_p) = C(F_1(Y_1), \dots, F_p(Y_p))$, where H is the joint cdf and F_i , $1 \leq i \leq p$ are the marginal cdf's for variables Y_1, \dots, Y_p . A natural extension to conditional distributions, the *conditional copula*, was initially used by Lambert and Vandenhende (2002) and subsequently formalized by Patton (2006) so that

$$H(Y_1, \dots, Y_p|X) = C(F_{1|X}(Y_1|X), \dots, F_{p|X}(Y_p|X)|X) \quad (1)$$

where $X \in R^q$ is a vector of conditioning variables. Clearly, the conditional copula is useful in regression models in which one may be interested in establishing the way the dependence structure itself, i.e. the copula, varies with the covariates. One possible approach that shows promise in applications is to consider a parametric copula C_θ and to allow the copula parameter θ (or a known transformation of θ) to vary as a function of X according to a function $\eta(X)$ which is called *the calibration function* by Acar et al. (2011).

Suppose we observe n independent measurements (Y_{1i}, Y_{2i}, X_i) , $i = 1 \dots n$, Y_{1i} and Y_{2i} in \mathbf{R} , X_i in \mathbf{R}^q . The likelihood for the conditional copula model is of the form

$$L = \prod_{i=1}^n f_1(Y_{1i}|X_i, \theta_1) f_2(Y_{2i}|X_i, \theta_2) c(F_1(Y_{1i}|X_i, \theta_1), F_2(Y_{2i}|X_i, \theta_2)|\theta(X_i)), \quad (2)$$

where F_1 and F_2 are conditional cumulative distribution functions with corresponding densities f_1 and f_2 and $c(u_1, u_2|\theta(X_i)) = \frac{\partial^2 C(u_1, u_2|\theta(X_i))}{\partial u_1 \partial u_2}$ is the copula density function with parameter $\theta(X_i)$ that contains all the information about the dependence between Y_{1i} and Y_{2i} when the covariate vector takes value X_i . Often, the parameter space of a copula is a subset of the real line, so we can write $g^{-1}(\theta(X)) = \eta(X)$ with $g(\cdot)$ a known one-to-one link function and $\eta(x) : \mathbf{R}^q \rightarrow \mathbf{R}$ the unknown calibration function of inferential interest.

Depending on the strength of assumptions we are willing to make about η , a number

of possible approaches are available. The most direct is to assume a known parametric form for the calibration function, e.g. constant or linear, and estimate the corresponding parameters by maximum likelihood estimation (Genest et al., 1995). This approach relies on having a reasonable idea about the shape of the calibration function which, in practice, tends to be unrealistic. A more flexible approach uses non-parametric methods (Acar et al., 2011; Veraverbeke et al., 2011) and estimate the calibration function using smoothing methods. For univariate X Craiu and Sabeti (2012) devised a Bayesian approach and for multivariate X we refer to Sabeti et al. (2014), Chavez-Demoulin and Vatter (2015) and Klein and Kneiß (2015). In all these papers the curse of dimensionality that appears even for moderate values of q , say $q > 3$, is avoided by specifying an additive model structure for the calibration function. However, little work has considered the case when an additive structure is not suitable. One exception is Hernández-Lobato et al. (2013) who used sparse GP prior for estimating the calibration function, but our numerical experiments showed that the q -dimensional Gaussian Process they used for calibration estimation may not capture important patterns for moderate sample size. Moreover, the full efficiency of their approach is hard to determine since they assume uniform marginals, a condition that is equivalent to knowing exactly the marginal distributions for the variables of interest. In fact, when the marginal distributions are estimated it is of paramount importance to account for the resulting variance inflation due to error propagation in the copula estimation. The Bayesian approach handles this issue automatically as long as one is able to study the full posterior distribution of all the parameters in the model, be they involved in the marginal or copula specification.

In this paper we assume that the marginal distributions are normals with constant variance and we assign Gaussian Process (GP) priors for the means of these distributions. The calibration function is assumed to have a GP prior that is evaluated at $\beta^T X$ for some normalized β , thus coupling the GP-prior with the *single index model (SIM)* of Choi et al. (2011) and Gramacy and Lian (2012). The GP-SIM is more flexible than a canonical linear model and computationally more manageable than a full GP with q variables. The proposed model can be used for large covariate dimension q and for large samples. Both marginal means will be fitted using sparse GP approaches so that large data sets can

be computationally manageable. The dimension reduction of the SIM approach has been noted also by Fermanian and Lopez (2015), but their method differs in fundamental aspects from the one proposed here.

So far, GP-SIM's have been used mostly in regression settings where the algorithm of Gramacy and Lian (2012) can be used to efficiently sample the posterior distribution. However, here the GP-SIM is embedded in a non-Gaussian likelihood which complicates the design of an efficient sampling algorithm.

In the next section we review the GP-SIM formulation and introduce the notation. Section 3 covers the conditional copula model, the computational algorithm and the model selection procedures proposed and in Section 4 we illustrate the efficiency of the method via simulation and real examples. The paper ends with conclusions and directions for future work.

2 Brief review of Bayesian inference for Sparse GP

We give a brief review of the GP properties that are relevant to this work (for more details, see Rasmussen, 2006; Titsias et al., 2008). Assume we observe data \mathcal{D} consisting of n independent pairs $\mathcal{D} = \{(x_i, y_i), i = 1 \dots n\}$, where $y_i \in \mathbf{R}$ and $x_i \in \mathbf{R}^q$. Suppose that the probability distribution of y_i has a known form and depends on x_i through some unknown function f , i.e.

$$P(Y_i|x_i) = P(Y_i|f(x_i)).$$

The goal is to estimate the unknown smooth function $f : \mathbf{R}^q \rightarrow \mathbf{R}$. We assign a Gaussian Process (GP) prior to the whole function f , i.e. we assume that:

$$(f(x_1), f(x_2), \dots, f(x_n))^T \sim \mathcal{N}(0, K(X, X; \mathbf{w})), \quad (3)$$

where $\mathcal{N}(\mu, \Sigma)$ denotes a multivariate normal distribution with mean μ and variance covariance matrix Σ and K is a covariance matrix which depends on x_1, \dots, x_n and additional parameters. In this paper we use the squared exponential kernel to model the matrix

$K(X, X; \mathbf{w})$, i.e. its (i, j) element is

$$k(x_i, x_j; \mathbf{w}) = e^{w_0} \exp \left[- \sum_{s=1}^{s=q} \frac{(x_{is} - x_{js})^2}{e^{w_s}} \right]. \quad (4)$$

The unknown parameters w_0, \dots, w_q that determine the strength of dependence in (4) are inferred from the data. This choice of kernel reflects our belief that the calibration functions do not exhibit sudden changes.

The contribution of the conditional copula model to the joint likelihood breaks the tractability of the posterior conditional densities and complicates the design of an efficient MCMC algorithm that can sample efficiently from the posterior distribution.

In addition, it has been known that the computational load of fitting a GP model becomes prohibitive when n is large since each MCMC update requires the calculation and inversion of the matrix $K(X, X; \mathbf{w}) \in \mathbf{R}^{n \times n}$. As a result, the full Bayesian analysis is manageable for small sample sizes, i.e. $n \approx 1000$. To make GP models applicable for larger data we follow the literature on *sparse GP* (more details can be found in Quiñero-Candela and Rasmussen, 2005; Snelson and Ghahramani, 2005; Naish-Guzman and Holden, 2007) in which it is assumed that learning about f can be achieved using a smaller sample of latent variables, called *inducing variables*, that channel the information contained in the covariates $\{x_1, \dots, x_n\}$. To complete the description we consider the following notation: if $X = (x_1, \dots, x_n)^T \in \mathbf{R}^{n \times q}$ and $X^* = (x_1^*, \dots, x_{n^*}^*)^T \in \mathbf{R}^{n^* \times q}$ then we denote $K(X, X^*; \mathbf{w}) \in \mathbf{R}^{n \times n^*}$ the matrix

$$K(X, X^*; \mathbf{w}) = \begin{bmatrix} k(x_1, x_1^*; \mathbf{w}) & \cdots & k(x_1, x_{n^*}^*; \mathbf{w}) \\ \vdots & \ddots & \vdots \\ k(x_n, x_1^*; \mathbf{w}) & \cdots & k(x_n, x_{n^*}^*; \mathbf{w}) \end{bmatrix}, \quad (5)$$

where $k(x_i, x_j^*; \mathbf{w})$ is defined as in (4). We also define the following two matrices that will be used throughout the paper

$$A(X^*, X; \mathbf{w}) = K(X^*, X, \mathbf{w})K(X, X, \mathbf{w})^{-1}, \quad (6)$$

$$B(X^*, X; \mathbf{w}) = K(X^*, X^*, \mathbf{w}) - K(X^*, X, \mathbf{w})K(X, X, \mathbf{w})^{-1}K(X^*, X, \mathbf{w})^T. \quad (7)$$

With this notation and if we abbreviate $f_i = f(x_i)$ then, following the GP definition, we obtain

$$\mathbf{f} = (f_1, f_2, \dots, f_n)^T \sim \mathcal{N}(0, K(X, X; \mathbf{w})). \quad (8)$$

In the next section we introduce the prior distribution of the unknown parameters \mathbf{w} . The conditional joint posterior distribution of the latent variables (\mathbf{f}) and parameters (\mathbf{w}) given the observed data \mathcal{D} does not have a tractable form and its study will require the use of Markov Chain Monte Carlo (MCMC) sampling methods. Specifically, we use Random Walk Metropolis (RWM) within Gibbs sampling for \mathbf{w} (Craiu and Rosenthal, 2014; Andrieu et al., 2003) while for \mathbf{f} we will use the elliptical slice sampling (Murray et al., 2010) that has been designed specifically for GP-based models and does not require tuning of free parameters.

The sparse GP approach relies on m pseudo-inputs through which we funnel the information contained in the observed data. The ratio m/n influences the trade-off between computational efficiency and statistical efficiency, as a smaller m will favour the former and a larger m will ensure no significant loss of the latter. If the m inducing or pseudo inputs are $\tilde{X} = (x_{u_1}, \dots, x_{u_m})^T \in \mathbf{R}^{m \times q}$ with corresponding function values $\tilde{\mathbf{f}} = (f(x_{u_1}), \dots, f(x_{u_m}))^T = (f_{u_1}, \dots, f_{u_m})^T$ where m is much smaller than n . The approximation links \mathbf{f} and $\tilde{\mathbf{f}}$ via

$$\pi(\mathbf{f}|\tilde{\mathbf{f}}) = A(X, \tilde{X}; \mathbf{w})\tilde{\mathbf{f}}, \quad (9)$$

where the matrix $A(X, \tilde{X}; \mathbf{w}) \in \mathbf{R}^{n \times m}$ is defined in (6). Since $\tilde{\mathbf{f}}$ completely determines \mathbf{f} , we can write joint density only in terms of m -dimensional vector $\tilde{\mathbf{f}}$

$$P(Y, \tilde{\mathbf{f}}, \mathbf{w}|X) = P(Y|A(X, \tilde{X}; \mathbf{w})\tilde{\mathbf{f}})\mathcal{N}(\tilde{\mathbf{f}}; 0, K(\tilde{X}, \tilde{X}; \mathbf{w}))P(\mathbf{w}). \quad (10)$$

The posterior distribution $\pi(\tilde{\mathbf{f}}, \mathbf{w}|\mathcal{D})$ is still of course not tractable and we need to use MCMC to study it, but the main advantage of this algorithm is that now we rely on calculating $K(X, \tilde{X}; \mathbf{w})$ which is just $n \times m$ matrix and $K(\tilde{X}, \tilde{X}; \mathbf{w})$ which is $m \times m$.

Given a new test point x^* we are interested in the corresponding distribution of $f^* =$

$f(x^*)$.

$$\begin{aligned} P(f^*|x^*, \mathcal{D}) &= \int P(f^*|\tilde{\mathbf{f}}, \mathbf{w}, x^*, \tilde{X})P(\tilde{\mathbf{f}}, \mathbf{w}|\mathcal{D})d\tilde{\mathbf{f}}d\mathbf{w} = \\ &= \int \mathcal{N}(f^*|A(x^*, \tilde{X}, \mathbf{w})\tilde{\mathbf{f}}, B(x^*, \tilde{X}, \mathbf{w}))P(\tilde{\mathbf{f}}, \mathbf{w}|\mathcal{D})d\tilde{\mathbf{f}}d\mathbf{w}. \end{aligned} \tag{11}$$

In general, the integral involved in (11) cannot be calculated in closed form but we can use posterior samples $(\tilde{\mathbf{f}}, \mathbf{w})^{(t)}$, $t = 1 \dots M$ to simulate

$$(f^*)^{(t)} \sim \mathcal{N}\left(A(x^*, \tilde{X}; \mathbf{w}^{(t)})\tilde{\mathbf{f}}^{(t)}, B(x^*, X, \mathbf{w}^{(t)})\right).$$

Statistical inference for $\pi(f^*|x^*, \mathcal{D})$ can be build based on samples $(f^*)^{(t)}$, $t = 1 \dots M$.

So far we have assumed that we know positions of inducing inputs \tilde{X} . Our approach is data-driven so we choose x_{u_1}, \dots, x_{u_m} as the centers of m clusters of original covariates X . We are using a simple k-means algorithm (Bishop, 2006) to create the clusters and locate these centers. The intuition is that we would like to have more inducing points in those regions that exhibit more variation in covariate values.

3 Conditional copula model formulation

Suppose that the observed data $\mathcal{D} = \{(Y_{1i}, Y_{2i}, x_i) \mid i = 1 \dots n\}$ consists of triplets (Y_{1i}, Y_{2i}, X_i) where $Y_{1i}, Y_{2i} \in \mathbf{R}$ and $X_i \in \mathbf{R}^q$. For notational convenience let $Y_1 = (Y_{11}, \dots, Y_{1n})^T$, $Y_2 = (Y_{21}, \dots, Y_{2n})^T$ and $X = (X_1, \dots, X_n)^T$. We assume that the marginal distribution of Y_{ji} ($j = 1, 2$) is Gaussian with mean $f_j(x_i)$ and constant variance σ_j^2 . If we let $\mathbf{f}_j = (f_j(x_1), \dots, f_j(x_n))^T$ we can compactly write:

$$P(Y_j|X) = \mathcal{N}(\mathbf{f}_j, \sigma_j^2 \mathbf{I}_n) \quad j = 1, 2 \tag{12}$$

We use a conditional copula to account for the fact that the dependence between the responses varies with covariate X . The likelihood is

$$P(Y_1, Y_2|X) = \prod_{i=1}^n \frac{1}{\sigma_1} \phi\left(\frac{Y_{1i} - \mathbf{f}_{1i}}{\sigma_1}\right) \frac{1}{\sigma_2} \phi\left(\frac{Y_{2i} - \mathbf{f}_{2i}}{\sigma_2}\right) \times \\ \times c\left(\Phi\left(\frac{Y_{1i} - \mathbf{f}_{1i}}{\sigma_1}\right), \Phi\left(\frac{Y_{2i} - \mathbf{f}_{2i}}{\sigma_2}\right) \mid \theta(x_i)\right) \quad (13)$$

Here c denotes a parametric copula density function, while Φ and ϕ are the cumulative probability function and density function of a standard normal distribution, respectively. The parameter of a copula depends on some unknown function $\theta(x_i) = g(f(x_i))$, where g is a known invertible link function that allows an unrestricted parameter space for \mathbf{f} . In this paper we assume that

$$f(x_i) = f(x_i^T \beta) \quad (14)$$

and set $\mathbf{f} = (f(x_1^T \beta), \dots, f(x_n^T \beta))^T$, where $\beta \in \mathbf{R}^d$ is normalized, i.e. $\|\beta\| = 1$ and $f : \mathbf{R} \rightarrow \mathbf{R}$ is an unknown function that is part of the inferential focus. Note that without normalization the parameter β is not identifiable. The *single index model (SIM)* defined by (14) has the advantage that it casts the original problem of estimating a general function f in q dimensions into a one-dimensional nonparametric and a q -dimensional parametric estimation. This dramatic reduction of complexity allows computational efficiency even for large sample sizes. The effect of model misspecification is studied via simulations in the next section.

The GP-SIM is fully specified once we assign the GP priors to f_1, f_2, f and the parametric priors for the remaining parameters, as follows:

$$f_1 \sim \mathcal{GP}(\mathbf{w}_1), \quad f_2 \sim \mathcal{GP}(\mathbf{w}_2), \quad f \sim \mathcal{GP}(\mathbf{w}), \\ \mathbf{w}_1 \sim \mathcal{N}(0, 5\mathbf{I}_{q+1}), \quad \mathbf{w}_2 \sim \mathcal{N}(0, 5\mathbf{I}_{q+1}), \quad \mathbf{w} \sim \mathcal{N}(0, 5\mathbf{I}_2), \\ \beta \sim \text{U}(S^{q-1}), \quad \sigma_1^2 \sim \mathcal{IG}(0.1, 0.1), \quad \sigma_2^2 \sim \mathcal{IG}(0.1, 0.1) \quad (15)$$

The $\mathcal{GP}(\mathbf{w})$ is a Gaussian Process prior with mean of 0, squared exponential kernel with parameters \mathbf{w} , $\text{U}(S^{q-1})$ is a uniform distribution on the surface of the q -dimensional unit sphere and $\mathcal{IG}(\alpha, \beta)$ denotes the inverse gamma distribution. One important thing to note

is that f_1 and f_2 are evaluated on \mathbf{R}^q while f is on \mathbf{R} . In order to avoid computational problems that affect the GP-based inference when the sample size is large, the inference will rely on the Sparse GP method that was described in the previous section. Suppose \tilde{X}_1 are m_1 inducing inputs for function f_1 , \tilde{X}_2 are m_2 inducing inputs for function f_2 and \tilde{Z} are m inducing inputs for function f . Also let $\tilde{\mathbf{f}}_1$ be f_1 evaluated at \tilde{X}_1 , $\tilde{\mathbf{f}}_2$ be f_2 evaluated at \tilde{X}_2 and $\tilde{\mathbf{f}}$ be f evaluated at \tilde{Z} . Then the joint density of the observed data and parameters is proportional to:

$$\begin{aligned}
P(Y_1, Y_2, \tilde{\mathbf{f}}_1, \tilde{\mathbf{f}}_2, \tilde{\mathbf{f}}, \mathbf{w}_1, \mathbf{w}_2, \mathbf{w}, \sigma_1^2, \sigma_2^2, \beta | X, \tilde{X}_1, \tilde{X}_2, \tilde{Z}) &\propto \mathcal{N}(Y_1; \mathbf{f}_1, \sigma_1^2 \mathbf{I}_n) \mathcal{N}(Y_2; \mathbf{f}_2, \sigma_2^2 \mathbf{I}_n) \times \\
&\times \prod_{i=1}^{i=n} c \left(\Phi \left(\frac{Y_{1i} - \mathbf{f}_{1i}}{\sigma_1} \right), \Phi \left(\frac{Y_{2i} - \mathbf{f}_{2i}}{\sigma_2} \right) | g(\mathbf{f}_i) \right) \mathcal{N}(\tilde{\mathbf{f}}_1; 0, K(\tilde{X}_1, \tilde{X}_1; \mathbf{w}_1)) \times \\
&\times \mathcal{N}(\tilde{\mathbf{f}}_2; 0, K(\tilde{X}_2, \tilde{X}_2; \mathbf{w}_2)) \mathcal{N}(\tilde{\mathbf{f}}; 0, K(\tilde{Z}, \tilde{Z}; \mathbf{w})) \mathcal{N}(\mathbf{w}_1; 0, 5\mathbf{I}_{q+1}) \times \\
&\times \mathcal{N}(\mathbf{w}_2; 0, 5\mathbf{I}_{q+1}) \mathcal{N}(\mathbf{w}; 0, 5\mathbf{I}_2) \mathcal{IG}(\sigma_1^2; 0.1, 0.1) \mathcal{IG}(\sigma_2^2; 0.1, 0.1),
\end{aligned} \tag{16}$$

where

$$\begin{aligned}
\mathbf{f}_1 &= A(X, \tilde{X}_1; \mathbf{w}_1) \tilde{\mathbf{f}}_1 \\
\mathbf{f}_2 &= A(X, \tilde{X}_2; \mathbf{w}_2) \tilde{\mathbf{f}}_2 \\
\mathbf{f} &= A(X\beta, \tilde{Z}; \mathbf{w}) \tilde{\mathbf{f}}.
\end{aligned} \tag{17}$$

The number of inducing inputs m_1 , m_2 and m can all be different but in our applications we will choose their values to be significantly smaller than the sample size, n . Ideally we need the number of inducing inputs to be as large as possible but at the same time make the MCMC implementation computationally feasible.

As suggested earlier we can define \tilde{X}_1 and \tilde{X}_2 as centers of m_1 and m_2 clusters of X . So if m_1 is the same as m_2 then inducing inputs would also be the same. We cannot use the same strategy for \tilde{Z} , since then we would need the centers for the clusters of the variable $X^T\beta$ which are unknown. If we assume that each covariate x_{ij} is between 0 and 1 (this can be achieved easily if we subtract the the minimum value and divide by range) then following the Cauchy-Schwartz inequality we obtain

$$\|x_i^T \beta\| \leq \sqrt{\|x_i\|^2 \|\beta\|^2} \leq \sqrt{q} \quad \forall x_i, \beta$$

Hence we can choose \tilde{Z} to be m equally spaced points in the interval $[-\sqrt{q}, \sqrt{q}]$.

3.1 Computational Algorithm

The crux of inference is the posterior distribution

$$\pi(\tilde{\mathbf{f}}_1, \tilde{\mathbf{f}}_2, \tilde{\mathbf{f}}, \mathbf{w}_1, \mathbf{w}_2, \mathbf{w}, \sigma_1^2, \sigma_2^2, \beta | \mathcal{D}, \tilde{X}_1, \tilde{X}_2, \tilde{Z}).$$

However, π is not mathematically tractable so the study of its properties will be based on a sample drawn using a MCMC algorithm. In this section we provide the detailed steps of the latter.

The general form of the algorithm falls within the class of Metropolis-within-Gibbs (MwG) samplers in which we update in turn each component of the chain by sampling from its conditional distribution, given all the other components. The presence of the copula in the likelihood breaks the usual conditional conjugacy of the GP models so none of the components have conditional distributions that can be sampled directly.

Suppose we are interested in sampling a target $\pi(\theta_1, \dots, \theta_k)$. A generic MwG sampler proceeds as follows:

Step I Initialize the chain at $\theta_1^{(1)}, \theta_2^{(1)}, \dots, \theta_k^{(1)}$.

Step R At iteration $t + 1$ run iteratively the following steps for each $j = 1, \dots, k$:

1. Sample $\theta_j^* \sim q_j(\theta_j | \theta_{-j}^{(t+1;t)})$ where $\theta_{-j}^{(t+1;t)} = (\theta_1^{(t+1)}, \dots, \theta_{j-1}^{(t+1)}, \theta_{j+1}^{(t)}, \dots, \theta_k^{(t)})$ is the most recent state of the chain with the first $j - 1$ components updated already (hence the supraindex $t + 1$), the j th component removed and the remaining $n - j$ components having the values determined at iteration t (hence the supraindex t).
2. Compute $r = \min \left\{ 1, \frac{\pi(\theta_1^{(t+1)}, \dots, \theta_{j-1}^{(t+1)}, \theta_j^*, \theta_{j+1}^{(t)}, \dots, \theta_k^{(t)}) q_j(\theta_j^{(t)} | \theta_{-j}^{(t+1;t)})}{\pi(\theta_1^{(t+1)}, \dots, \theta_{j-1}^{(t+1)}, \theta_j^*, \theta_{j+1}^{(t)}, \dots, \theta_k^{(t)}) q_j(\theta_j^* | \theta_{-j}^{(t+1;t)})} \right\}$.
3. With probability r accept proposal and set $\theta_j^{(t+1)} = \theta_j^*$ and with $1 - r$ reject proposal and let $\theta_j^{(t+1)} = \theta_j^{(t)}$.

The proposal density $q_j(\cdot | \cdot)$ corresponds to the transition kernel used for the j th component. Our algorithm uses a number of proposals corresponding to Random Walk

Metropolis-within-Gibbs (RWMwG), Independent Metropolis-within-Gibbs (IMwG) and Elliptical Slice Sampling within Gibbs (SSwG) moves.

At the $t + 1$ step we use the following proposals to update the chain:

\mathbf{w}_i : Use a RWM transition kernel: $\mathbf{w}^* \sim \mathcal{N}(\mathbf{w}_i^{(t)}, c_{w_i} \mathbf{I}_{d+1})$. The constant c_{w_i} is chosen so that the acceptance rate is about 30%, $i = 1, 2$.

\mathbf{w} : Use the RWM: $\mathbf{w}^* \sim \mathcal{N}(\mathbf{w}^{(t)}, c_w \mathbf{I}_2)$. The constant c_w is chosen so that the acceptance rate is about 30%.

σ_i^2 : Without the copula, the conditional posterior distribution of σ_i^2 would be $\mathcal{IG}(0.1 + n/2, 0.1 + (Y_i - A_i \tilde{\mathbf{f}}_i^{(t)})^T (Y_i - A_i \tilde{\mathbf{f}}_i^{(t)}))$ where $A_i = A(X, \tilde{X}_i; \mathbf{w}_i^{(t+1)})$ for all $i = 1, 2$. We will use this distribution as a proposal distribution in the IM transition kernel, i.e. the proposal is $(\sigma_i^2)^* \sim \mathcal{IG}(0.1 + n/2, 0.1 + (Y_i - A_i \tilde{\mathbf{f}}_i^{(t)})^T (Y_i - A_i \tilde{\mathbf{f}}_i^{(t)}))$. The acceptance rate is usually in the range of $[0.25, 0.60]$ and the chain mixes better than it would under a RWM.

β : Since β is normalized we will use RWM on unit sphere using ‘Von-Mises-Fisher’ distribution (henceforth denoted \mathcal{VMF}). The VMF distribution has two parameters, μ (normalized to have norm 1) which represents the mean direction and κ , the concentration parameter. A larger κ implies that the distribution will be more concentrated around μ . The density is symmetric in μ and the argument and is proportional to $f_{VMF}(x; \mu, \kappa) \propto \exp(\kappa x^T \mu)$.

The proposals are generated using $\beta^* \sim \mathcal{VMF}(\beta^{(t)}, \kappa)$, where κ is chosen so that the acceptance rate is around 30%.

$\tilde{\mathbf{f}}$'s: For $\tilde{\mathbf{f}}_i$, $i = 1, 2$ and $\tilde{\mathbf{f}}$ we use the elliptical slice sampling proposed by Murray et al. (2010) which does not require the tuning of simulation parameters.

In our experience the efficiency of the algorithm benefits from initial values that are not too far from the posterior mode. Therefore we propose first to estimate the two independent regressions for Y_1 and Y_2 to get $(\tilde{\mathbf{f}}_1, \mathbf{w}_1, \sigma_1^2)^{(1)}$ and $(\tilde{\mathbf{f}}_2, \mathbf{w}_2, \sigma_2^2)^{(1)}$. Then run another MCMC fixing marginals and only sampling $(\tilde{\mathbf{f}}, \mathbf{w})$. This procedure estimates $(\tilde{\mathbf{f}}, \mathbf{w})^{(1)}$. These 3

short chains (100-200 iterations each) give point-estimates of true parameters and these estimates can be used as initial values for the joint MCMC. This simple approach shortens the time it would take for the original chain to find the regions of high mass under the posterior.

Empirically we have also found, that for faster convergence it is better to start with small w_1 values (allowing for more variation in the calibration function). If the chain starts in large w_1 values, it requires a large number of simulations before it moves to the correct region in the sample space.

3.2 Model Selection

The conditional copula model involves two types of selection. First one needs to choose the copula family, presumably from a set of possible candidates. Second, it is often of interest to determine whether a parametric simple form for the calibration is supported by the data. For instance, a constant calibration function indicates that the dependence structure does not vary with the covariates, a conclusion that may be of scientific interest in some applications. We investigate the performance of three measures of fit that can be estimated from the MCMC samples $\omega^{(t)}$ $t = 1 \dots M$ where $\omega^{(t)}$ is the vector of parameters and latent variables drawn at step t from the posterior corresponding to model \mathcal{M} .

3.3 Cross-Validated Pseudo Marginal Likelihood

The cross-validated pseudo marginal likelihood (CVML) (Geisser and Eddy, 1979; Hanson et al., 2011) calculates the average (over parameter values) prediction power for model \mathcal{M} via

$$\text{CVML}(\mathcal{M}) = \sum_{i=1}^n \log(P(Y_{1i}, Y_{2i} | \mathcal{D}_{-i}, \mathcal{M})), \quad (18)$$

where \mathcal{D}_{-i} is the data set from which the i th observation has been removed. A direct calculation of CVML would be impractical if we were required to sample from n posteriors each corresponding to samples of size $n - 1$. This is not the case because one can show (see, for example, Sabeti et al., 2014) that if we denote by ω all the parameters and latent

variables in the model, then

$$E [P(Y_{1i}, Y_{2i}|\omega, \mathcal{M})^{-1}] = P(Y_{1i}, Y_{2i}|\mathcal{D}_{-i}, \mathcal{M})^{-1}, \quad (19)$$

where the expectation is with respect to conditional (posterior) distribution of ω given full data \mathcal{D} and the model \mathcal{M} . Based on the posterior samples we can estimate the CVML as

$$\text{CVML}_{est}(\mathcal{M}) = - \sum_{i=1}^n \log \left(\frac{1}{M} \sum_{t=1}^M P(Y_{1i}, Y_{2i}|\omega^{(t)}, \mathcal{M})^{-1} \right) \quad (20)$$

and the model with the largest CVML is selected.

3.4 Conditional CVML criterion

We also propose a novel extension of CVML which we call conditional CVML (CCVML). Since the copula construction is particularly useful in predicting one response given the other ones, we explore this feature by computing the predictive distribution of one response given the rest of the data. More precisely, instead of calculating the marginal probability of a pair (Y_{1i}, Y_{2i}) given all the other observations, \mathcal{D}_{-i} , we find the probabilities $P(Y_{1i}|Y_{2i}, \mathcal{D}_{-i})$ and $P(Y_{2i}|Y_{1i}, \mathcal{D}_{-i})$ using

$$\text{CCVML}(\mathcal{M}) = \frac{1}{2} \left\{ \sum_{i=1}^n \log [P(Y_{1i}|Y_{2i}, \mathcal{D}_{-i}, \mathcal{M})] + \sum_{i=1}^n \log [P(Y_{2i}|Y_{1i}, \mathcal{D}_{-i}, \mathcal{M})] \right\}. \quad (21)$$

Note that when the marginal distributions are uniform, then CCVML is the same as CVML.

One can show using a technique similar to the one used in Sabeti et al. (2014) that

$$\begin{aligned} E [P(Y_{1i}|Y_{2i}, \omega, \mathcal{M})^{-1}] &= E \left[\frac{P(Y_{2i}|\omega, \mathcal{M})}{P(Y_{1i}, Y_{2i}|\omega, \mathcal{M})} \right] = P(Y_{1i}|Y_{2i}, \mathcal{D}_{-i}, \mathcal{M})^{-1} \\ E [P(Y_{2i}|Y_{1i}, \omega, \mathcal{M})^{-1}] &= E \left[\frac{P(Y_{1i}|\omega, \mathcal{M})}{P(Y_{1i}, Y_{2i}|\omega, \mathcal{M})} \right] = P(Y_{2i}|Y_{1i}, \mathcal{D}_{-i}, \mathcal{M})^{-1}. \end{aligned} \quad (22)$$

Based on (22) one can easily estimate CCVML from MCMC samples:

$$\text{CCVML}_{est}(\mathcal{M}) = -\frac{1}{2} \sum_{i=1}^n \left\{ \log \left[\frac{1}{M} \sum_{t=1}^M \frac{P(Y_{2i}|\omega^{(t)}, \mathcal{M})}{P(Y_{1i}, Y_{2i}|\omega^{(t)}, \mathcal{M})} \right] + \log \left[\frac{1}{M} \sum_{t=1}^M \frac{P(Y_{1i}|\omega^{(t)}, \mathcal{M})}{P(Y_{1i}, Y_{2i}|\omega^{(t)}, \mathcal{M})} \right] \right\}. \quad (23)$$

3.5 Deviance Information Criterion

The Deviance Information Criterion (DIC, Spiegelhalter et al., 2002) is widely used in Bayesian inference. It consists of a measure of fit

$$\text{fit}(\mathcal{M}) = \log P(\mathcal{D}|E[\omega], \mathcal{M}) \quad (24)$$

and ‘effective number of parameters’ which can be calculated in two different ways as suggested by Spiegelhalter et al. (2002) and Gelman et al. (2014), respectively

$$\begin{aligned} p_1(\mathcal{M}) &= 2(\text{fit}(\mathcal{M}) - E[\log P(\mathcal{D}|\omega, \mathcal{M})]) \\ p_2(\mathcal{M}) &= 2\text{Var}[\log P(\mathcal{D}|\omega, \mathcal{M})]. \end{aligned} \quad (25)$$

Expectations and variance are with respect to the posterior distribution of ω given data and model. DIC is then formally defined as

$$\text{DIC}_j(\mathcal{M}) = -2\text{fit}(\mathcal{M}) + 2p_j(\mathcal{M}) \quad j = 1, 2 \quad (26)$$

The MCMC estimates of the above quantities based on posterior samples can be easily obtained, for example:

$$\text{fit}_{est}(\mathcal{M}) = \log P \left(\mathcal{D} \left| \frac{\sum_{t=1}^{t=M} \omega^{(t)}}{M}, \mathcal{M} \right. \right) \quad (27)$$

Similarly, estimates of ‘effective number of parameters’ and DIC can be calculated.

The model with smallest DIC is selected.

3.6 Watanabe-Akaike Information Criterion

Watanabe-Akaike Information Criterion (WAIC, Watanabe, 2010; Gelman et al., 2014) is another model selection tool in Bayesian statistics which avoids some problems that DIC has. However WAIC is applicable only for observations that are independent given parameters (which is true for GP-SIM). As with DIC, we start with measure of fit

$$\text{fit}(\mathcal{M}) = \sum_{i=1}^{i=N} \log E [P(y_{1i}, y_{2i}|\omega, \mathcal{M})] \quad (28)$$

and two ways to define penalties

$$\begin{aligned} p_1(\mathcal{M}) &= 2 \left(\text{fit}(\mathcal{M}) - \sum_{i=1}^{i=N} E[\log P(y_{1i}, y_{2i}|\omega, \mathcal{M})] \right) \\ p_2(\mathcal{M}) &= \sum_{i=1}^{i=N} \text{Var}[\log P(y_{1i}, y_{2i}|\omega, \mathcal{M})]. \end{aligned} \quad (29)$$

As in DIC all expectations and variance are with respect to the posterior distribution of ω , WAIC is defined as

$$\text{WAIC}_j(\mathcal{M}) = -2\text{fit}(\mathcal{M}) + 2p_j(\mathcal{M}) \quad j = 1, 2 \quad (30)$$

The MCMC estimate of the fit is found using the following expression

$$\text{fit}_{est}(\mathcal{M}) = \sum_{i=1}^{i=N} \log \left(\frac{\sum_{t=1}^{t=M} P(y_{1i}, y_{2i}|\omega^{(t)}, \mathcal{M})}{M} \right) \quad (31)$$

Similarly p_j and WAIC_j $j = 1, 2$ can be estimated. The model with smallest WAIC is selected.

We use the CVML, DIC and WAIC criteria not only for copula selection but also to select a known functional form for the calibration function.

4 Performance of the algorithms

4.1 Simulations

The purpose of the simulation study is to assess empirically: 1) the performance of the estimation method under the correct and misspecified models, as well as 2) the ability of the model selection criteria to identify the correct copula structure, i.e. the copula family and the parametric form of the calibration function. For the former aim we compute the integrated mean square for various quantities of interest, including the Kendall's tau. In order to facilitate estimation performance across different copula families, we estimate the calibration function on the Kendall's τ scale. The latter is given by

$$\tau(X) = 4 \left(\iint C(U_1, U_2|X)c(U_1, U_2|X)dU_1dU_2 \right) - 1. \quad (32)$$

We will compare 3 copulas: Clayton, Frank and Gaussian under the general GP-SIM model and the Clayton with constant calibration function. To fit the model with constant copula, we still use MCMC but instead of $\mathbf{f}, \tilde{\mathbf{f}}, \mathbf{w}$ and β in calibration we have a constant scalar copula parameter, θ . The RWMwG transition is used to sample θ , as the proposal distributions for marginals' parameters and latent variables remain the same.

Table 1 provides inverse-link functions for calibration and Kendall's tau formulas in terms of copula parameters. In addition of Kendall's tau we use also the conditional mean

Copula	Inv-Link function	Kendall's tau formula
Clayton	$\theta = \exp(f) - 1$	$\tau = \frac{\theta}{\theta+2}$
Frank	$\theta = f$	No closed form
Gaussian	$\rho = \frac{\exp(f)-1}{\exp(f)+1}$	$\tau = \frac{2}{\pi} \arcsin \rho$

Table 1: Inv-links and Kendall's tau formulas

of Y_1 given Y_2 and X for assessing the estimation. Such conditional means can be useful in prediction when one of the responses is more expensive to measure than the other. The calculation is mathematically straightforward

$$E(Y_1|Y_2 = y_2, X = x) = f_1(x) + \sigma_1 \int_0^1 \Phi^{-1}(z)c \left(z, \Phi \left(\frac{y_2 - f_2(x)}{\sigma_2} \right); \theta(x) \right) dz. \quad (33)$$

If we assume that marginal distributions are uniform then we have the simpler expression:

$$E(U_1|U_2 = u_2, X = x) = \int_0^1 c(z, u_2; \theta(x)) dz \quad (34)$$

The integrals in (33) and (34) are usually not tractable, but can be easily estimated via numerical integration since they are one-dimensional and defined on the closed interval $[0, 1]$.

4.2 Simulation Details

We generate samples of size $n = 400$ from each of the next 5 scenarios using the Clayton copula. The covariates are generated independently from $U(0, 1)$ distribution. In scenarios 1, 2 and 3 covariate dimension d is 2, in scenarios 4 and 5, the dimension is 5.

Sc1 $f_1(x) = 0.6 \sin(5x_1) - 0.9 \sin(2x_2)$,
 $f_2(x) = 0.6 \sin(3x_1 + 5x_2)$,
 $\tau(x) = 0.7 + 0.15 \sin(15x^T \beta)$
 $\beta = (1, 3)^T / \sqrt{10}$, $\sigma_1 = \sigma_2 = 0.2$

Sc2 $f_1(x) = 0.6 \sin(5x_1) - 0.9 \sin(2x_2)$
 $f_2(x) = 0.6 \sin(3x_1 + 5x_2)$
 $\tau(x) = 0.3 \sin(5x^T \beta)$
 $\beta = (1, 3)^T / \sqrt{10}$, $\sigma_1 = \sigma_2 = 0.2$

Sc3 $f_1(x) = 0.6 \sin(5x_1) - 0.9 \sin(2x_2)$
 $f_2(x) = 0.6 \sin(3x_1 + 5x_2)$
 $\tau(x) = 0.5$
 $\sigma_1 = \sigma_2 = 0.2$

Sc4 $f_1(x) = f_2(x) = 0.7(\sin(3x_1) - \sin(3x_2) + \sin(3x_3) - \sin(3x_4) + \sin(3x_5))$
 $\tau(x) = 0.8 + 0.10 \sin(10x_1x_2) - 0.20(x_3x_4 - 0.5)^2 - 0.20x_5$
 $\sigma_1 = \sigma_2 = 0.2$

$$\begin{aligned}
\mathbf{Sc5} \quad f_1(x) &= f_2(x) = 0.7(\sin(3x_1) - \sin(3x_2) + \sin(3x_3) - \sin(3x_4) + \sin(3x_5)) \\
\tau(x) &= 0.1 + 0.20 \sin(10x_1x_2) - 0.20(x_3x_4 - 0.5)^2 - 0.20x_5 \\
\sigma_1 &= \sigma_2 = 0.2
\end{aligned}$$

Sc1 and **Sc2** have calibration functions for which the SIM model is true for Kendall’s tau and, consequently, also for calibration function. **Sc1** corresponds to large dependence (τ greater than 0.5) while **Sc2** has small dependence (τ is between -0.3 and 0.3). In the scenarios in which $d = 2$ we use $m = 20$ inducing inputs for all the sparse GP procedures (marginals and copula) and for higher dimensions ($d = 5$) we still used $m = 20$ inducing points for the calibration estimation but increased to $m = 30$ inducing inputs for the marginals since higher dimensional estimation requires more inputs. The case **Sc3** corresponds to the covariate-free dependence ($\tau = 0.5$) and allows us to verify the selection criterias’ power to detect simple parametric forms for the calibration. Scenarios **Sc4** and **Sc5** do not have SIM form and will be useful to evaluate the effect of model misspecification on the inference. Again one of them corresponds to high dependence ($\tau \in [0.5, 0.9]$) and another to small one ($\tau \in [-0.3, 0.3]$).

Markov Chain Monte Carlo was run for 5000 iterations with only the last 3000 iterations used for inference. As noted earlier, starting values were found by running two GP regressions separately to estimate marginal parameters and one MCMC sampler was run in order to estimate calibration parameters. All three samplers were run for only 100 iterations.

The simulation results show that **Sc1** and **Sc2** performed similarly. Since the calibration function in **Sc1** is more complicated, for the sake of reducing the paper’s length we present only results for that scenario. The trace-plots, autocorrelation functions and histograms of posterior samples of β , σ_1^2 and σ_2^2 are shown in Figure 1 when the copula belongs to the correct Clayton family (red line is the true value). Next we show predictions for the marginals means with 95% credible intervals. Since these are 2-dimensional we estimate ‘slices’ from this surface at values 0.2 and 0.8, so that we first fix $x_1 = 0.2$ then $x_1 = 0.8$ and similarly for x_2 . The results are in Figure 2 (black is true, green is estimation, red are credible intervals).

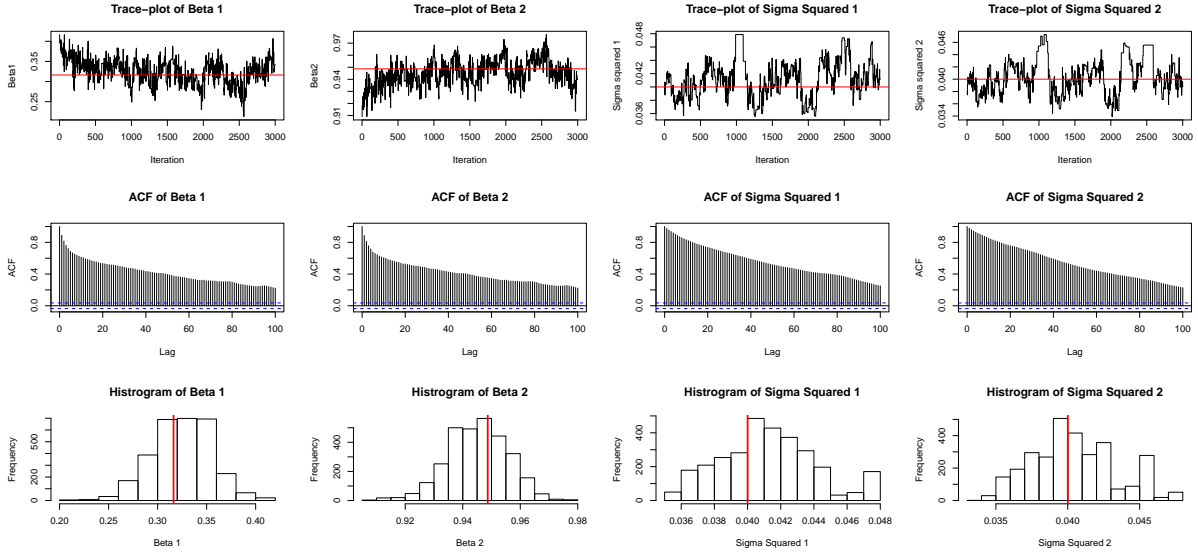


Figure 1: **Sc1**: Trace-plots, ACFs and histograms of parameters based on MCMC samples generated under the true Clayton family.

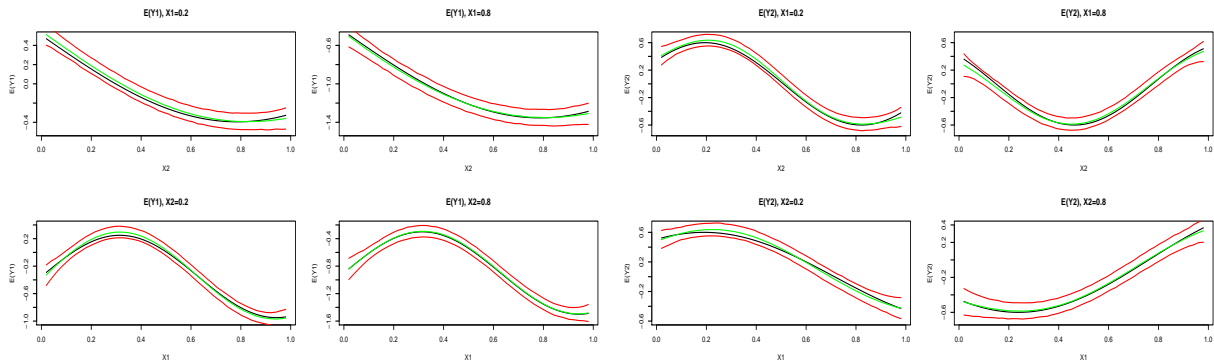


Figure 2: **Sc1**: Estimation of Marginal means. The leftmost 2 columns show the accuracy for predicting Y_1 and the rightmost 2 columns show the results for predicting Y_2 . The black and green lines represent the true and estimated relationships, respectively. The red lines are the limits of the pointwise 95% credible intervals obtained under the true Clayton family.

One of the inferential goals is the prediction of calibration function or, equivalently, Kendall's tau function. In this case we are dealing with only two covariates so their joint effect can be visualized via the calibration surface. In Figure 3 we show the true calibration surface on the left panel and the fitted one on the right. The accuracy is remarkable and we are hard put to see major differences between the two panels.

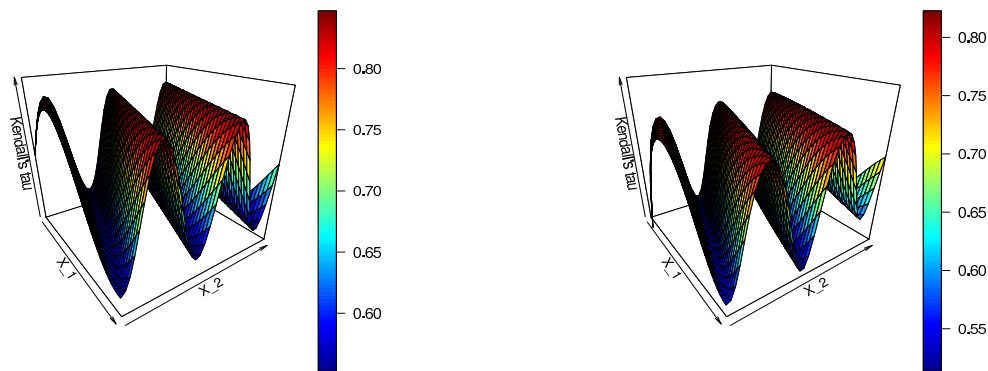


Figure 3: **Sc1**: Estimation of Kendall's tau dependence surface. The true surface (left panel) is very similar to the estimated one (right panel).

Since the visual comparison of the three-dimensional true and fitted surfaces may be misleading, we also estimate one dimensional slices at values 0.2 and 0.8 and the results, shown in Figure 4, confirm the accuracy of the fit.

Another way to evaluate how well the model makes predictions is to fix 4 covariate points and estimate corresponding Kendall's tau values: $\hat{\tau}(0.2, 0.2)$, $\hat{\tau}(0.2, 0.8)$, $\hat{\tau}(0.8, 0.2)$, $\hat{\tau}(0.8, 0.8)$. At each MCMC iteration these predictions are calculated and histograms (Figure 5) are constructed (red lines are true value of τ). The same estimates are presented in Figure 6 when the Gaussian copula is used for inference. One can notice that the estimates are biased in this instance, thus emphasizing the importance of identifying correctly the right copula family. Similar patterns have been observed when using the Frank copula.

Finally, we focus on the accuracy of CVML, DIC and WAIC in selecting the correct model. Table 2 shows the values for each scenario and model. Bold values indicate largest CVML and smallest DIC/WAIC values for each scenario.

Observe that all bold values for **Sc1**, **Sc2**, **Sc4**, **Sc5**, are in Clayton row, while for **Sc3** they are in Clayton-constant section, it means that for each scenario CVML, DIC and WAIC selected the right model.

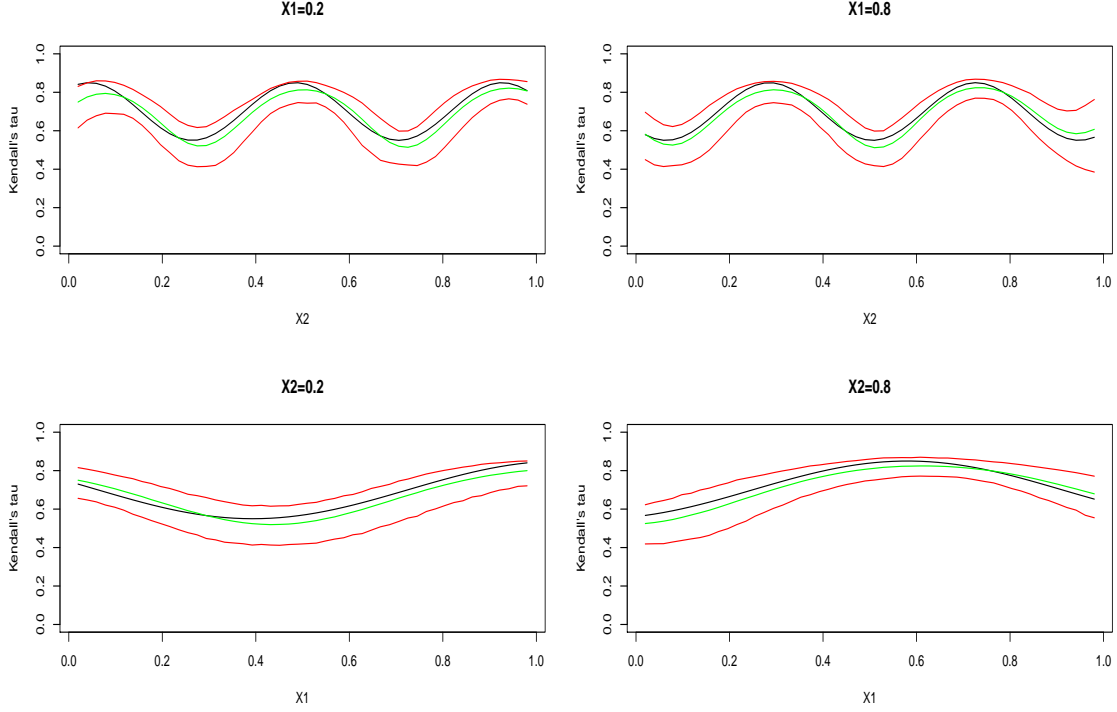


Figure 4: **Sc1**: Estimation of Kendall's tau one-dimensional projections when $X_1 = 0.2$ or 0.8 (top panels) and when $X_2 = 0.2$ or 0.8 bottom panels. The black and green lines represent the true and estimated relationships, respectively. The red lines are the limits of the pointwise 95% credible in intervals obtained under the true Clayton family.

	CVML	CCVML	DIC ₁	DIC ₂	WAIC ₁	WAIC ₂		CVML	CCVML	DIC ₁	DIC ₂	WAIC ₁	WAIC ₂
Scenario 1							Scenario 4						
Clayton	496	417	-995	-949	-999	-994	Clayton	502	423	-1021	-995	-1013	-1005
Frank	435	362	-874	-876	-874	-870	Frank	450	378	-910	-859	-907	-900
Gaussian	405	329	-826	-807	-822	-817	Gaussian	455	379	-920	-914	-918	-915
Clayton-Const	455	378	-913	-885	-914	-910	Clayton-Const	492	419	-987	-985	-988	-984
Scenario 2							Scenario 5						
Clayton	166	103	-332	-317	-335	-333	Clayton	157	105	-323	-303	-322	-316
Frank	144	82	-290	-242	-292	-289	Frank	145	98	-292	-281	-295	-290
Gaussian	146	84	-294	-255	-296	-293	Gaussian	150	102	-305	-296	-305	-303
Clayton-Const	121	60	-244	-245	-246	-243	Clayton-Const	140	92	-279	-274	-278	-285
Scenario 3													
Clayton	322	254	-645	-609	-647	-644							
Frank	277	209	-557	-526	-551	-549							
Gaussian	276	207	-555	-540	-551	-547							
Clayton-Const	323	255	-648	-625	-650	-647							

Table 2: CVML, CCVML, DIC and WAIC values for each Scenario and Model

So far out plots have been based on a single implementation of the method. In order to facilitate interpretation, we perform 50 independent replications under each of the five scenarios described previously. However, since the focus of the inference is on the copula,

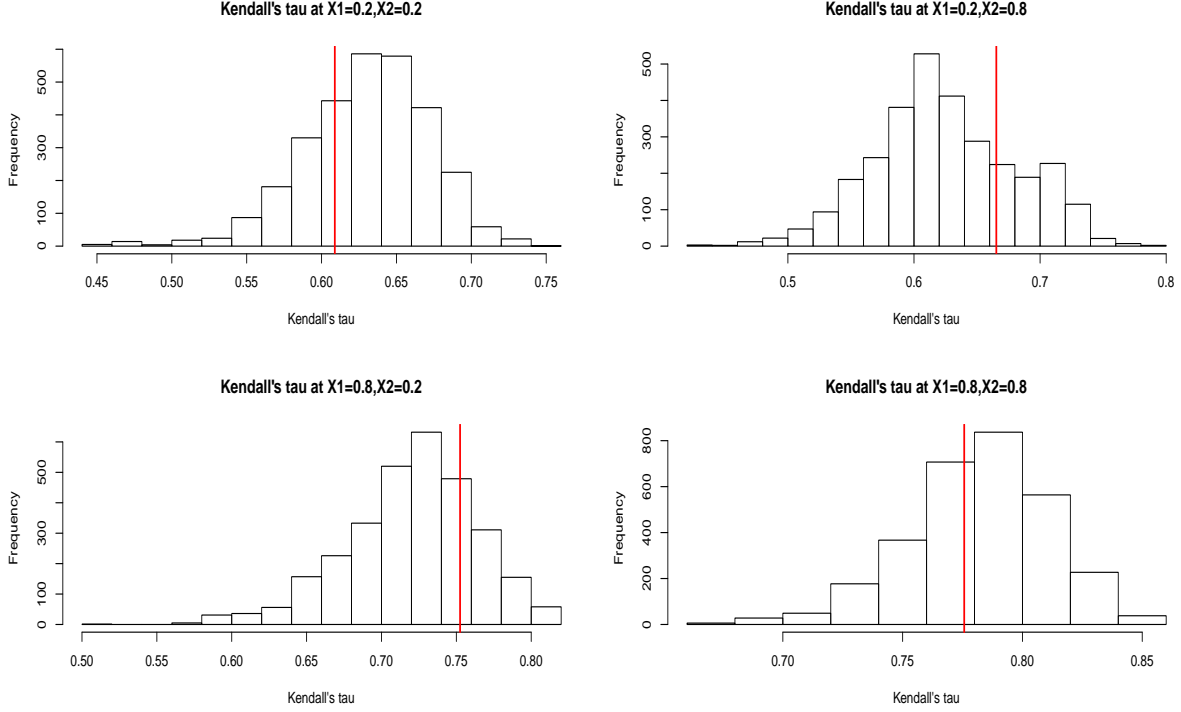


Figure 5: **Sc1**: Histogram of predicted Kendall's τ values obtained under the true Clayton copula.

we will simplify the simulations by assuming that the marginals are uniform.

The MCMC sampler was run for 3000 iterations and first 1000 were discarded. For each data set, 4 estimations were done with Clayton, Frank, Gaussian and constant Clayton copulas. The goal is to estimate integrated squared Bias (IBias²), Variance (IVar) and mean squared error (IMSE) of Kendall's tau evaluated at covariates $X = (x_1, \dots, x_n)^T$. To calculate these quantities for any scenario and any model we do the following: for each data set, point estimations are produced $\hat{\tau}_r(x_i)$ where r runs from 1 up to number of replicates (R) and $i = 1 \dots n$. The formulas for IBias², IVar and IMSE are given by:

$$\begin{aligned}
 \text{IBias}^2 &= \sum_{i=1}^{i=n} \left(\frac{\sum_{r=1}^{r=R} \hat{\tau}_r(x_i)}{R} - \tau(x_i) \right)^2 / n \\
 \text{IVar} &= \sum_{i=1}^{i=n} \text{Var}_r(\hat{\tau}_r(x_i)) / n \\
 \text{IMSE} &= \text{IBias}^2 + \text{IVar}
 \end{aligned} \tag{35}$$

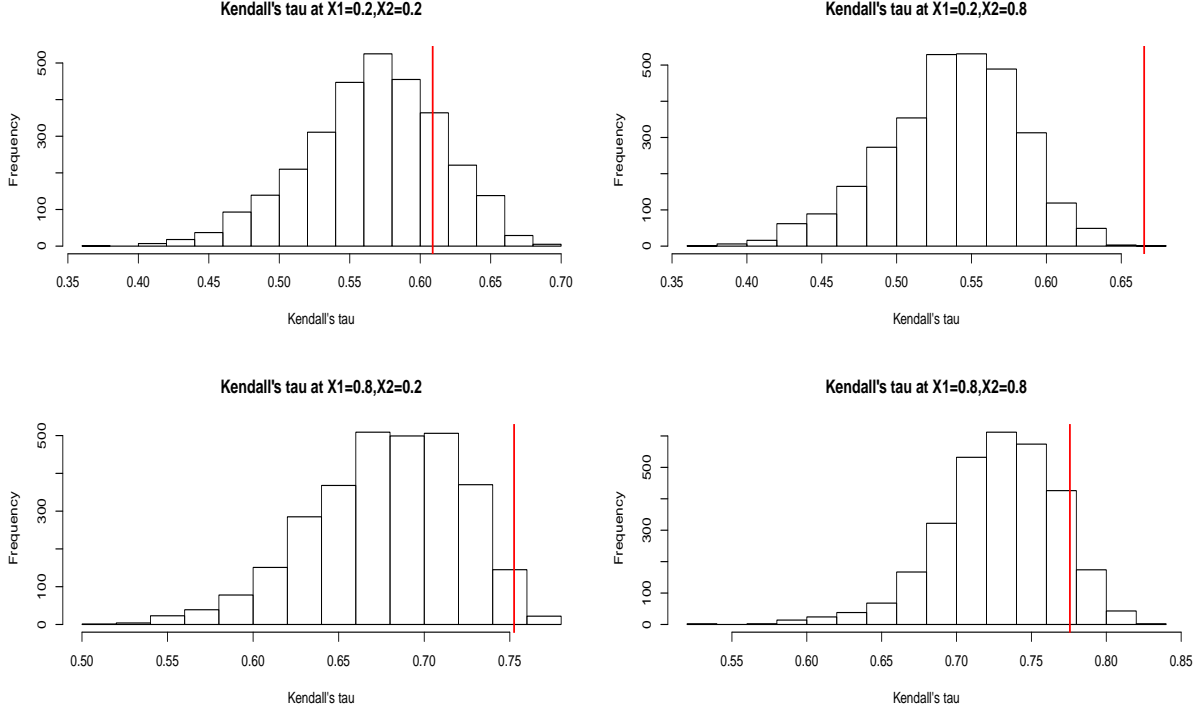


Figure 6: **Sc1**: Histogram of predicted τ_s (Gaussian copula)

We will apply these concepts not only for Kendall's taus but also for $E(U_1|U_2 = u_2, X = x)$ for different u_2 and x combinations. Here we use U s instead of Y s to indicate that we assume uniform marginal distributions.

Results

IBias², IVar and IMSE for each scenario and each model are shown in Table 3 (bold values show smallest IMSE for each scenario). First we note that the smallest IMSE is produced

Scenario	Clayton			Frank			Gaussian			Clayton Constant		
	$\sqrt{\text{IBias}^2}$	$\sqrt{\text{IVar}}$	$\sqrt{\text{IMSE}}$									
Sc1	0.0223	0.0556	0.0599	0.0491	0.0714	0.0867	0.0664	0.0741	0.0995	0.1071	0.0133	0.1079
Sc2	0.0160	0.0576	0.0598	0.0839	0.0938	0.1258	0.0383	0.0738	0.0832	0.2208	0.0304	0.2229
Sc3	0.0061	0.0318	0.0324	0.0300	0.0467	0.0555	0.0483	0.0552	0.0734	0.0028	0.0116	0.0119
Sc4	0.0285	0.0463	0.0544	0.0384	0.0631	0.0738	0.0621	0.0787	0.1003	0.1003	0.0124	0.1011
Sc5	0.0518	0.0578	0.0777	0.0749	0.0901	0.1172	0.0569	0.0762	0.0951	0.1003	0.0234	0.1030

Table 3: Estimated $\sqrt{\text{Bias}^2}$, $\sqrt{\text{IVar}}$ and $\sqrt{\text{IMSE}}$ of Kendall's tau for each Scenario and Model

with true model. Also IMSE of **Sc4** is comparable with **Sc1** even though calibration function of **Sc4** is not a single index.

For each simulated data set and each model, $E(U_1|U_2 = u_2, X = x)$ were estimated. For **Sc1**, **Sc2** and **Sc3** we set each x_1, x_2, u_2 to take values from $\{0.2, 0.4, 0.6, 0.8\}$, making a total of 64 combinations. For **Sc4** and **Sc5**, we made $u_2 \in \{0.2, 0.4, 0.6, 0.8\}$ and 25 points from $[0, 1]^5$ that span covariate space, so that we had a total of 100 combinations. The results are presented in Table 4.

Scenario	Clayton			Frank			Gaussian			Clayton Constant		
	$\sqrt{\text{IBias}^2}$	$\sqrt{\text{IVar}}$	$\sqrt{\text{IMSE}}$									
Sc1	0.0038	0.0131	0.0137	0.0279	0.0132	0.0309	0.0338	0.0163	0.0375	0.0237	0.0034	0.0240
Sc2	0.0034	0.0145	0.0149	0.0256	0.0310	0.0403	0.0226	0.0184	0.0292	0.0644	0.0084	0.0649
Sc3	0.0015	0.0070	0.0072	0.0265	0.0076	0.0275	0.0346	0.0122	0.0367	0.0007	0.0028	0.0029
Sc4	0.0117	0.0083	0.0144	0.0240	0.0109	0.0264	0.0362	0.0145	0.0390	0.0162	0.0031	0.0165
Sc5	0.0426	0.0125	0.0444	0.0480	0.0262	0.0547	0.0427	0.0158	0.0455	0.0435	0.0067	0.0441

Table 4: Estimated IBias^2 , IVar and IMSE of $E(U_1|U_2, X)$ for each Scenario and Model

Finally we show how well CVML, DIC and WAIC perform in choosing correct model. For selecting between different copula families or to check whether dependence is covariate-free we just pick the model with largest CVML or smallest DIC/WAIC. Table 5 shows how often Clayton model is selected over other models using CVML, DIC and WAIC for **Sc1**, **Sc2**, **Sc4** and **Sc5**. Similarly Table 6 shows how often Clayton-constant is selected over other models for **Sc3**.

Scenario	Frank					Gaussian					Clayton Constant				
	CVML	DIC ₁	DIC ₂	WAIC ₁	WAIC ₂	CVML	DIC ₁	DIC ₂	WAIC ₁	WAIC ₂	CVML	DIC ₁	DIC ₂	WAIC ₁	WAIC ₂
Sc1	100%	100%	98%	100%	100%	100%	100%	98%	100%	100%	98%	98%	96%	98%	98%
Sc2	100%	100%	100%	100%	100%	100%	100%	100%	100%	100%	100%	100%	100%	100%	100%
Sc4	100%	100%	100%	100%	100%	100%	100%	100%	100%	100%	100%	100%	100%	100%	100%
Sc5	96%	90%	86%	98%	96%	100%	98%	72%	100%	100%	88%	100%	32%	94%	90%

Table 5: The percentage of correct decisions for each selection criterion when comparing the correct Clayton model with a non-constant calibration with all the other models: Frank model with non-constant calibration, Gaussian model with non-constant calibration, Clayton model with non-constant calibration. Notice that the CCVML and the CVML criteria are exactly equal in the case in which the marginals are uniform.

If we first look at selecting between Clayton and constant Clayton, WAIC_2 and CVML are the best model selection measures. DIC_2 performs very poorly, because in these examples, it has largest penalty (among DIC_1 and WAIC) for non-constant copulas. Therefore

Scenario	Clayton					Frank					Gaussian				
	CVML	DIC ₁	DIC ₂	WAIC ₁	WAIC ₂	CVML	DIC ₁	DIC ₂	WAIC ₁	WAIC ₂	CVML	DIC ₁	DIC ₂	WAIC ₁	WAIC ₂
Sc3	78%	64%	88%	70%	78%	100%	100%	100%	100%	100%	100%	100%	100%	100%	100%

Table 6: The percentage of correct decisions for each selection criterion when comparing the correct Clayton model with a constant calibration with all the other models: Clayton model with non-constant calibration, Frank model with non-constant calibration and the Gaussian model with non-constant calibration. Notice that the CCVML and the CVML criterions are exactly equal in the case in which the marginals are uniform.

DIC₂ selects constant copula more frequently than GP-SIM, making more errors.

To select between copula families CVML, WAIC₁ and WAIC₂ on average work better than DICs.

4.3 Weather Data

Data from 500 weather stations across North America at 6AM (EST) on August 25, 2015 were downloaded from ‘Openweathermap’ website ¹. We consider how dependence between temperature and humidity changes with latitude, longitude and wind speed. For each model the MCMC was run for 6000 iterations with 2000 burn-in period, 30 inducing inputs were used for the marginals and calibration function estimation ($m_1 = m_2 = m = 30$). The resulting CVML, DIC and WAIC values are shown in Table 7.

	Clayton	Frank	Gaussian	Gumbel	T-3	T-5
CVML	-1069	-934	-1019	-1129	-955	-960
CCVML	-505	-364	-448	-565	-383	-393
DIC ₁	2116	1832	1976	2231	1886	1884
DIC ₂	2186	1890	2012	2291	1916	1965
WAIC ₁	2142	1852	1995	1899	1899	1908
WAIC ₂	2140	1868	2029	2262	1914	1922

Table 7: Weather data: CVML, DIC and WAIC criteria values different models

All model selection measures indicate that the among the candidate models the most suitable one is the Frank copula. The GP-SIM coefficients fitted under the Frank copula model are shown in Table 8.

Based on these results one may be able to conclude that the covariate ‘Latitude’ can

¹<http://openweathermap.com>

Variable	Posterior Mean	95% Credible Interval
Latitude	0.0280	$[-0.1895, 0.1950]$
Longitude	0.9670	$[0.9141, 0.9960]$
Wind	-0.2095	$[-0.3997, -0.0023]$

Table 8: Posterior means and quantiles of β

be eliminated from the model. However, when we computed all the criteria for the models without “Latitude” they all pointed to having this covariate included in the model. An important observation is that model adequacy requires that if the covariate is omitted from the copula model it must be omitted also from the marginals (Patton, 2006; Acar et al., 2011). Despite not having a strong effect on the copula parameter, the “Latitude” covariate must be included because it has an important effect on one or both of the marginals.

Figure 7 shows 3 plots of Kendall’s tau calibration curves with 95% credible intervals by fixing two covariates at mid-range values and varying the third one. On this particular day, the longitude seems to exhibit the highest level of variation when latitude is fixed at its mid-range value which is approximately 50° North. At that latitude we follow the US-Canada border on the Canadian side. The plot reflects the widely different relationships between temperature and humidity in the West and East coast and the very clear regime change around the Canadian Rockies. The relatively constant effect of wind is not surprising given the low speeds recorded. It is also interesting to notice that latitude also seems to play little effect, along the -95° W longitude. This is not surprising one we notice that at this longitude we cross Manitoba and western Ontario in Canada and mostly flat states in US (Iowa, Minnesota, Missouri, Arkansas and Texas) which tend to exhibit similar patterns in the summer.

In order to demonstrate the difficulty one would have in gauging the complex evolution of dependence between temperature and humidity as a function of the latitude and longitude we plot in Figure 8 the response variables together as they vary with longitude and latitude. It is clear that the model manages to identify a pattern that would be very difficult to distinguish without the help of a flexible mathematical model.

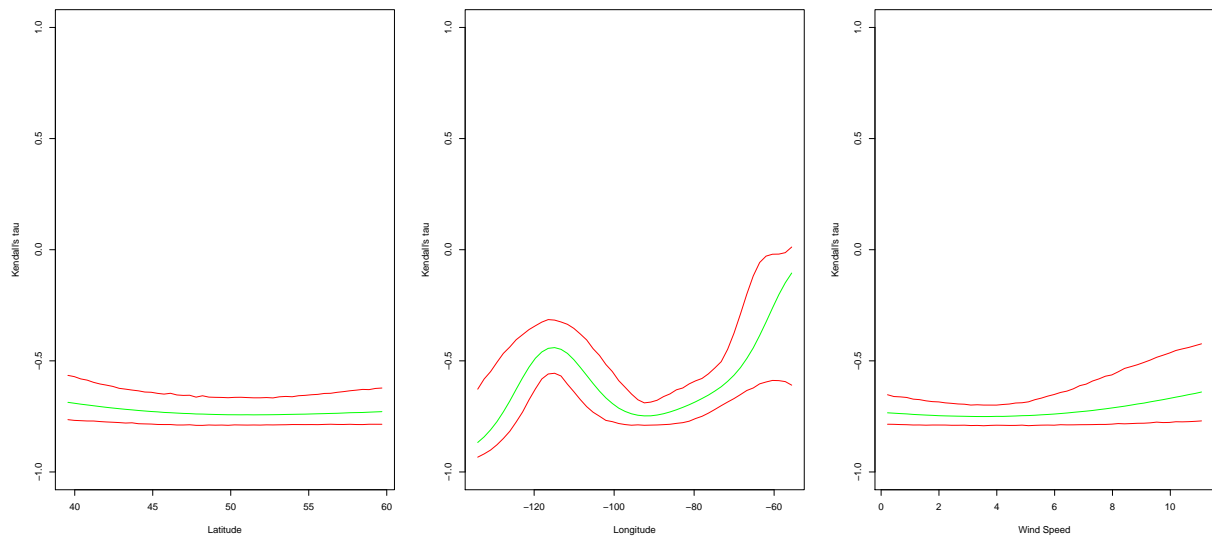


Figure 7: Weather Data: One-dimensional slices of Kendall's tau. Left Panel: Latitude varies, Middle Panel: Longitude varies, Right Panel: Wind Speed varies.

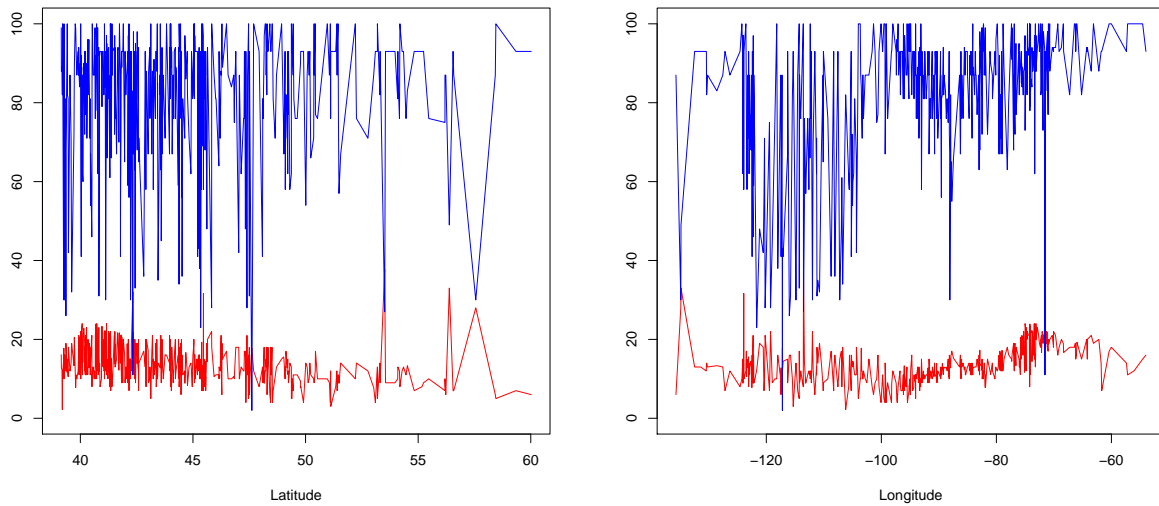


Figure 8: Weather Data: Plots of temperature (red) and humidity (blue) against latitude (left panel) and longitude (right panel).

5 Conclusion

We propose a Bayesian procedure to estimate the calibration function of a conditional copula model jointly with the marginal distributions. In our attempt to move away from an additive model hypothesis we consider a sparse Gaussian process priors used in conjunction with a single index model. The resulting procedure avoids the curse of dimensionality for small and moderate covariate dimension and can be implemented in large sample sizes. The selection of copulas and comparison between a constant and non-constant calibrations is performed via a number of selection criteria. We introduce a novel conditional cross-validated marginal likelihood predictive criterion for both copula selection and for comparing a constant and non-constant calibration functions. The performance of the model is illustrated using simulated and real data.

An important development we are currently investigating concerns implementing this approach in more complex settings in which a higher number of dependent variables requires the use of vine copulas (Aas et al., 2009; Min and Czado, 2010).

Acknowledgement

Funding support of this work was provided by the the Natural Sciences and Engineering Research Council of Canada and the Canadian Statistical Sciences Institute.

References

- AAS, K., CZADO, C., FRIGESSI, A. and BAKKEN, H. (2009). Pair-copula constructions of multiple dependence. *Insurance Mathematics & Economics* **44** 182–198.
- ACAR, E. F., CRAIU, R. V. and YAO, F. (2011). Dependence calibration in conditional copulas: A nonparametric approach. *Biometrics* **67** 445–453.
- ANDRIEU, C., DE FREITAS, N., DOUCET, A. and JORDAN, M. I. (2003). An introduction to MCMC for machine learning. *Machine learning* **50** 5–43.

- BISHOP, C. M. (2006). *Pattern recognition and machine learning*. Springer-Verlag New York Inc. pringer.
- CHAVEZ-DEMOULIN, V. and VATTER, T. (2015). Generalized additive models for conditional copulas. *J. Multivariate Anal.* **141** 147–167. Preprint.
- CHOI, T., SHI, J. Q. and WANG, B. (2011). A Gaussian process regression approach to a single-index model. *Journal of Nonparametric Statistics* **23** 21–36.
- CRAIU, R. V. and ROSENTHAL, J. S. (2014). Bayesian computation via Markov chain Monte Carlo. *Annual Review of Statistics and Its Application* **1** 179–201.
- CRAIU, R. V. and SABETI, A. (2012). In mixed company: Bayesian inference for bivariate conditional copula models with discrete and continuous outcomes. *Journal of Multivariate Analysis* **110** 106–120.
- FERMANIAN, J.-D. and LOPEZ, O. (2015). Single-index copulae. ArXiv preprint: 1512.07621.
- GEISSER, S. and EDDY, W. F. (1979). A predictive approach to model selection. *Journal of the American Statistical Association* **74** 153–160.
- GELMAN, A., HWANG, J. and VEHTARI, A. (2014). Understanding predictive information criteria for bayesian models. *Statistics and Computing* **24** 997–1016.
- GENEST, C., GHOUDI, K. and RIVEST, L.-P. (1995). A semiparametric estimation procedure of dependence parameters in multivariate families of distributions. *Biometrika* **82** 543–552.
- GRAMACY, R. B. and LIAN, H. (2012). Gaussian process single-index models as emulators for computer experiments. *Technometrics* **54** 30–41.
- HANSON, T., BRANSCUM, A. and JOHNSON, W. (2011). Predictive comparison of joint longitudinal-survival modelling: a case study illustrating competing approaches. *Lifetime Data Analysis* **17** 2–28.

- HERNÁNDEZ-LOBATO, J. M., LLOYD, J. R. and HERNÁNDEZ-LOBATO, D. (2013). Gaussian process conditional copulas with applications to financial time series. In *Advances in Neural Information Processing Systems*.
- KLEIN, N. and KNEISS, T. (2015). Simultaneous inference in structured additive conditional copula regression models: a unifying Bayesian approach. *Stat. Comput.* 1–20.
- LAMBERT, P. and VANDENHENDE, F. (2002). A copula-based model for multivariate non-normal longitudinal data: analysis of a dose titration safety study on a new antidepressant. *Statist. Medicine* **21** 3197–3217.
- MIN, A. and CZADO, C. (2010). Bayesian inference for multivariate copulas using pair-copula constructions. *Journal of Financial Econometrics* **8** 511–546.
- MURRAY, I., ADAMS, R. P. and MACKAY, D. J. (2010). Elliptical slice sampling. In *International Conference on Artificial Intelligence and Statistics*.
- NAISH-GUZMAN, A. and HOLDEN, S. (2007). The generalized FITC approximation. In *Advances in Neural Information Processing Systems*.
- PATTON, A. J. (2006). Modelling asymmetric exchange rate dependence*. *International economic review* **47** 527–556.
- QUIÑONERO-CANDELA, J. and RASMUSSEN, C. E. (2005). A unifying view of sparse approximate Gaussian process regression. *The Journal of Machine Learning Research* **6** 1939–1959.
- RASMUSSEN, C. E. (2006). Gaussian processes for machine learning .
- SABETI, A., WEI, M. and CRAIU, R. V. (2014). Additive models for conditional copulas. *Stat* **3** 300–312.
- SKLAR, A. (1959). Fonctions de répartition à n dimensions et leurs marges. *Publications de l’Institut de Statistique de l’Université de Paris* **8** 229–231.
- SNELSON, E. and GHAHRAMANI, Z. (2005). Sparse Gaussian processes using pseudo-inputs. In *Advances in neural information processing systems*.

- SPIEGELHALTER, D. J., BEST, N. G., CARLIN, B. P. and VAN DER LINDE, A. (2002). Bayesian measures of model complexity and fit. *Journal of the Royal Statistical Society: Series B (Statistical Methodology)* **64** 583–639.
- TITSIAS, M. K., LAWRENCE, N. and RATTRAY, M. (2008). Markov chain Monte Carlo algorithms for Gaussian processes. *Inference and Estimation in Probabilistic Time-Series Models* 9.
- VERAVERBEKE, N., OMELKA, M. and GIJBELS, I. (2011). Estimation of a conditional copula and association measures. *Scand. J. Statist.* to appear.
- WATANABE, S. (2010). Asymptotic equivalence of Bayes cross validation and widely applicable information criterion in singular learning theory. *The Journal of Machine Learning Research* **11** 3571–3594.